Dyes and Pigments 99 (2013) 489–495

Contents lists available at SciVerse ScienceDirect

Dyes and Pigments

journal homepage: www.elsevier.com/locate/dyepig

Structural and spectral characterizations of C.I. Disperse Blue 148 having a new crystalline form

Hui-Fen Qian [a,b], Yin-Ge Wang [b], Xiao-Chun Chen [a], Wei-Gang Ruan [c], Wei Huang [a,*]

[a] State Key Laboratory of Coordination Chemistry, Nanjing National Laboratory of Microstructures, School of Chemistry and Chemical Engineering, Nanjing University, Nanjing, Jiangsu Province 210093, PR China
[b] College of Sciences, Nanjing University of Technology, Nanjing, Jiangsu Province 210009, PR China
[c] Zhejiang YUTAI Hi-Tech Chemical Co., Ltd., №. 113, Shengli East Road, Shaoxing, Zhejiang Province 312000, PR China

ARTICLE INFO

Article history:
Received 22 April 2013
Received in revised form
30 May 2013
Accepted 2 June 2013
Available online 18 June 2013

Keywords:
Azo dye
C.I. Disperse Blue 148
Crystalline form
Powder X-ray diffraction
π–π Stacking
Hydrogen bonding

ABSTRACT

Single-crystal structures of the best high-temperature trichromatic blue azo dye C.I. Disperse Blue 148 and its diazonium component 3-amino-5-nitro-[2,1]- benzisothiazole are described herein. C.I. Disperse Blue 148 exhibits an essentially coplanar molecular structure and a dimeric packing mode between adjacent phenyl and benzisothiazole rings. Particularly, PXRD measurement reveals the existence of a new crystalline form of C.I. Disperse Blue 148 having the highest melting point and the best thermal stability, which is obviously different from all the known α, β, and γ forms. A one-phase recrystallization method, which can guarantee the complete transformation, is used to prepare the new crystalline form instead of the conventional heating of an aqueous suspension of α form. Furthermore, TGA–DSC and pH titration experiments have been carried out to reveal the thermal and pH stabilities of this heterocyclic dye. To our knowledge, this is the first structural example on benzisothiazole involved azo dyes.

1. Introduction

Recently, aromatic heterocycle azo dyes have attracted much attention because most of them generally have large molar extinction coefficients and show brilliant color and high chromophoric strength and fastness [1–4]. The design and development of new aromatic heterocycle disperse azo dyes have become one hot research area in modern textile chemistry [5,6]. In our previous work, several Disperse Yellow azo dyes crystallizing in the hydrazone form in the solid state and their azo-hydrazone tautomerisms driven by pH titration and metal-ion complexation have been investigated [7–14]. Additionally, we have studied four heterocyclic Disperse Red azo dyes having the same benzothiazole/azo/benzene skeleton [15].

C.I. Disperse Blue 148, which was firstly announced in a German patent from the BASF company in 1965 [16] and involved in another US patent as one component of a series of dye compositions [17], is a representative aromatic heterocycle monoazo blue dye exhibiting excellent wet fastness and compatibility with other dyes. In 1973, the BASF company declared in a UK patent [18] the existence of α, β, and γ forms of C.I. Disperse Blue 148, which have been confirmed by the powder X-ray diffraction (PXRD) measurements. Up to now, it is still widely used as one of the primary colors in high-temperature dyeing and high-temperature steaming for printing, which has achieved the best applications in cellulose acetate fibers, especially in the textile discharge printing. Moreover, C.I. Disperse Blue 148 is a halide-free blue dye, which is environmentally friendly, showing extraordinary thermal stability and basic hydrolizing properties [19,20].

In general, the fibers are sensitive to the reductants and bases in the process of discharge printing, and the control of the temperature and the amount of base is very important [21]. So it is of high value to investigate the structural and spectral properties of C.I. Disperse Blue 148 because of the above-mentioned advantages of this special dye, in particular its thermal and pH stabilities [22]. In this work, we have carried out the X-ray single-crystal structure, PXRD, thermal analysis and pH titration of a new crystalline form of C.I. Disperse Blue 148, which is obviously different from all the known α, β, and γ forms. By checking the latest version of CCDC database (updated to August 2012), it is found that C.I. Disperse Blue 148 is the first structural example on benzisothiazole based azo dyes, so we also include the single-crystal structure of its diazonium component 3-amino-5-nitro- [2,1]-benzisothiazole in this work to give an intuitionistic comparison.

* Corresponding author. Tel.: +86 25 83686526; fax: +86 25 83314502.
E-mail address: whuang@nju.edu.cn (W. Huang).

0143-7208/$ – see front matter © 2013 Elsevier Ltd. All rights reserved.
http://dx.doi.org/10.1016/j.dyepig.2013.06.002

Table 1
Crystal and structural refinement data for C.I. Disperse Blue 148 and **1**.

Compound	C.I. Disperse Blue 148	**1**
Empirical formula	$C_{19}H_{19}N_5O_4S$	$C_7H_5N_3O_2S$
Formula weight	413.46	195.20
Temperature/K	291(2)	291(2)
Wavelength/Å	0.71073	0.71073
Crystal size (mm)	0.10 × 0.12 × 0.14	0.16 × 0.14 × 0.12
Crystal system	Monoclinic	Monoclinic
Space group	$P2_1/c$	Pn
a/Å	11.936(1)	3.733(1)
b/Å	21.026(2)	8.567(1)
c/Å	7.697(1)	12.425(2)
α/°	90	90
β/°	94.520(2)	97.267(3)
γ/°	90	90
V/Å^3	1926(3)	394.18(11)
Z/D_{calcd} (g/cm^3)	4/1.426	2/1.645
F(000)	864	200
μ/mm^{-1}	0.206	0.375
h_{min}/h_{max}	−14/14	−4/4
k_{min}/k_{max}	−25/25	−10/7
l_{min}/l_{max}	−9/9	−14/14
Data/parameters	10,463/265	2111/118
Flack	–	−0.05(13)
Final R indices[$I > 2\delta(I)$]	$R1 = 0.0870$	$R1 = 0.0445$
	$wR2 = 0.1981$	$wR2 = 0.1065$
R indices(all data)	$R1 = 0.1487$	$R1 = 0.0476$
	$wR2 = 0.2269$	$wR2 = 0.1080$
S	1.083	1.032
Max./min. $\Delta\rho$/e·Å^{-3}	0.522/−0.265	0.270/−0.338

$R1 = \Sigma||Fo|-|Fc||/\Sigma|Fo|$, $wR2 = [\Sigma[w(Fo^2-Fc^2)^2]/\Sigma w(Fo^2)^2]^{1/2}$.

2. Experimental section

2.1. Materials and measurements

Melting point was measured without corrections. The reagents of analytical grade were purchased from commercial sources and used without any further purification. UV–vis spectra were recorded with a Shimadzu UV-2700 double-beam spectrophotometer using a quartz glass cell with a path length of 10 mm. Infrared (IR) spectra (4000–400 cm^{-1}) were recorded using a Nicolet FT-IR 170X spectrophotometer on KBr disks. ^{1}H NMR spectra were measured with a Bruker dmx500 MHz NMR spectrometer at room temperature. Powder X-ray diffraction measurements were performed on a Philips X'pert MPD Pro X-ray diffractometer using Cu Kα radiation (λ = 0.15418 nm), in which the X-ray tube was operated at 40 kV and 40 mA at room temperature. All pH measurements were made with a pH-10 C digital pH meter. TGA–DSC (thermogravimetry analysis–differential scanning calorimeter) experiments were carried out by a NETZSCH STA449C thermogravimetric analyzer instrument in the nitrogen flow from10 to 600 °C at a heating rate of 5.0 °C/min.

2.2. Recrystallization from the α form to the crystalline form of C.I. Disperse Blue 148

The α form of C.I. Disperse Blue 148 (0.10 g) was dissolved in 25 mL ethanol in a round-bottom flask under heating, and then distilled water (15 mL) was added dropwise under reflux to prepare a saturated solution of C.I. Disperse Blue 148. The hot solution was filtered quickly, and the filtrate was cooled to 0 °C. The solid was collected by filtration, washed by a cold mixture of ethanol and distilled water (5:3, v/v) and dried in a vacuum. Main FT-IR absorptions (KBr pellets, ν, cm^{-1}): 3415 (w), 1735 (vs), 1596 (s), 1319 (s), 1122 (s), 1074 (m) and 815 (m). *Anal.* calcd for $C_{19}H_{19}N_5O_4S$: C, 55.19; H, 4.63; N, 16.94%. Found: C, 55.11; H, 4.71; N, 17.02%. ^{1}H NMR (500 MHz, $CDCl_3$, ppm): δ 9.18 (s, 1H, benzisothiazole), 8.20 (dd, 1H, J = 2.2 Hz, J = 9.6 Hz, benzisothiazole), 7.97 (d, 2H, J = 9.1 Hz, phenyl), 7.75 (d, 1H, J = 9.6 Hz, benzisothiazole), 6.79 (d, 2H, J = 7.2 Hz, phenyl), 3.81 (t, 2H, NCH_2), 3.74 (s, 3H, OCH_3), 3.58 (q, 2H, NCH_2), 2.71 (t, 2H, CH_2), 1.28 (t, 3H, CH_3).

Table 2
Selected bond distances (Å) and angles (°) for C.I. Disperse Blue 148 and **1**.

Bond distances		Bond angles	
C.I. Disperse Blue 148			
S1–N2	1.642(5)	N2–S1–C7	97.5(3)
S1–C7	1.683(6)	C16–O3–C17	115.7(5)
O1–N1	1.223(6)	O1–N1–O2	122.4(6)
O2–N1	1.225(6)	O1–N1–C2	119.3(5)
O3–C16	1.301(7)	O2–N1–C2	118.3(5)
O3–C17	1.471(8)	S1–N2–C5	108.0(4)
O4–C16	1.194(8)	N4–N3–C7	112.6(5)
N1–C2	1.441(8)	N3–N4–C8	113.8(5)
N2–C5	1.332(8)	C11–N5–C14	119.1(5)
N3–N4	1.277(6)	C11–N5–C18	124.2(5)
N3–C7	1.376(7)	C14–N5–C18	116.7(5)
N4–C8	1.394(7)		
N5–C11	1.358(7)		
N5–C14	1.459(8)		
N5–C18	1.490(8)		
1			
C1–N1	1.320(5)	N1–C1–C2	127.5(3)
C1–S1	1.721(4)	C2–C1–S1	107.3(3)
C3–N2	1.337(5)	N2–S1–C1	96.6 (2)
N2–S1	1.679(3)		

2.3. X-ray data collection and solution

Single-crystal samples of C.I. Disperse Blue 148 and 3-amino-5-nitro-[2,1]-benzisothiazole (**1**) were covered in glue and mounted on glass fibers for data collection on a Bruker SMART 1K CCD area detector at 291(2) K, respectively, using graphite mono–chromated Mo Kα radiation (λ = 0.71073 Å). The collected data were reduced by using the program SAINT [23] and empirical absorption corrections were done by SADABS [24] program. The crystal systems were determined by Laue symmetry and the space groups were assigned on the basis of systematic absences by using XPREP. The structures were solved by direct method and refined by least-squares method. All non-hydrogen atoms were refined on F^2 by full-matrix least-squares procedure using anisotropic displacement parameters, while hydrogen atoms were inserted in the calculated positions assigned fixed isotropic thermal parameters at 1.2 times of the equivalent isotropic U of the atoms to which they are attached (1.5 times for the methyl groups) and allowed to ride on their respective parent atoms. All calculations were carried out on a PC with the SHELXTL PC program package [25] and molecular graphics were drawn by using XSHELL, Diamond and ChemBio-Draw softwares. The summary of the crystal data, experimental details and refinement results for C.I. Disperse Blue 148 and **1** is listed in Table 1. Selected bond distances and bond angles of C.I. Disperse Blue 148 and **1** are given in Table 2, while intermolecular hydrogen bonding interactions are listed in Table 3.

Table 3
Hydrogen bonding parameters (Å, °) in C.I. Disperse Blue 148 and **1**.

D–H···A	D–H	H···A	D···A	∠DHA	Symmetry code
C.I. Disperse Blue 148					
C13–H13···O4	0.93	2.57	3.422(8)	152	$1-x, -y, 1-z$
C14–H14B···O2	0.97	2.52	3.310(9)	138	$1-x, -y, 1-z$
1					
N1– H1A···N2	0.86	2.09	2.948(5)	172	$-1/2+x, 1-y, -1/2+z$
N1 –H1B···O2	0.86	2.08	2.882(5)	154	$1+x, y, z$

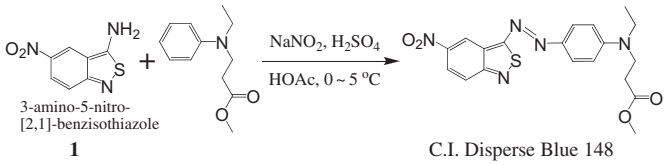

Scheme 1. Schematic illustration for the preparation of C.I. Disperse Blue 148.

3. Results and discussion

3.1. Synthesis, new crystalline form and spectral characterizations of C.I. Disperse Blue 148

C.I. Disperse Blue 148 was prepared *via* the conventional diazotization and the coupling reactions between 3-amino-5-nitro-[2,1]-benzisothiazole and *N*-ethyl-*N*-2-(methoxycarbonyl)ethyl-aniline, as shown in Scheme 1. The compound was first obtained as the α form (black line in Fig. 1) with a melting point of 83–87 °C, which is the same as that described in the BSAF patent. And then it was purified by the column chromatography (silica gel, toluene-ethylacetate, 1:1, v/v) and recrystallization from ethanol. It is worthwhile to mention that further experiments reveal that only a simple one-phase recrystallization from a mixture of ethanol and water can produce successfully the pure compound of C.I. Disperse Blue 148.

The microcrystal of C.I. Disperse Blue 148 has a melting point of 117–119 °C which is higher than all the previously reported ones [26]. The blue and yellow single crystals of C.I. Disperse Blue 148 and **1** suitable for X-ray diffraction measurement were both obtained from a mixture of acetonitrile and ethanol (v:v = 1:1) by slow evaporation in air at room temperature for one week.

The pure phase of C.I. Disperse Blue 148 is confirmed by the PXRD patterns, where the experimental curve (the blue line in Fig. 1) is in good agreement with the simulative one (the red line in Fig. 1). It should be mentioned that a new crystalline form of C.I. Disperse Blue 148 had been observed, which is obviously different from all the known α, β, and γ forms. Actually, our new crystalline form exhibits the best baseline, resolution and intensity in the same

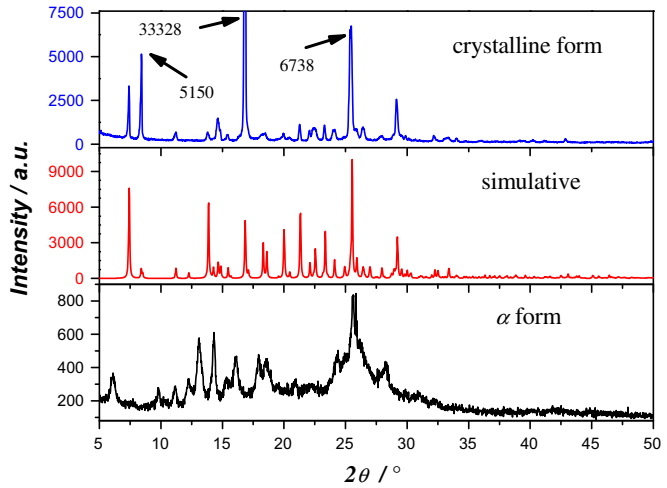

Fig. 1. The simulative (the middle red line) and experimental (the top blue line for the new crystal form and the bottom black line for the α form) PXRD patterns for C.I. Disperse Blue 148. The intensity of three strongest peaks is shown for the new crystalline form at the diffraction angles (2θ) of 8.4, 16.8 and 25.5°. (For interpretation of the references to color in this figure legend, the reader is referred to the web version of this article.)

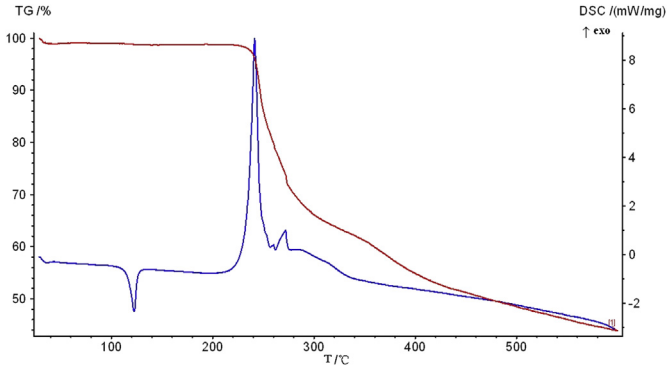

Fig. 2. TGA–DSC diagram of C.I. Disperse Blue 148.

experimental condition compared with the known α, β, and γ forms. The PXRD measurement of C.I. Disperse Blue 148 indicates a very strong peak at a diffraction angle 2θ [°] of 16.8 with the intensity of 33,328. The second strongest peak at $2\theta = 25.5°$ (6738) is comparable with the strongest peak at $2\theta = 25.6$, 25.3 and 24.5° in the α, β and γ forms [18]. However, the third strongest peak at $2\theta = 8.4°$ (5150) for the crystalline form of C.I. Disperse Blue 148 is a new one.

The TGA–DSC study of C.I. Disperse Blue 148 reveals that it has no weight loss until 210 °C, as can be seen in Fig. 2, and after that it begins to decompose with a sharp exothermic DSC peak at 217 °C. However, there is a melting process below 201 °C, which is evidenced by an endothermic DSC peak at 121 °C.

From the methods claimed in the UK patent, the transformation from α form to β form of C.I. Disperse Blue 148 need the heating of an aqueous suspension at 60–85 °C for eight hours, which should be divided into three stages at different temperature ranges. In contrast, the produce of γ form of C.I. Disperse Blue 148 need heating the aqueous suspension of α form at 70–95 °C for eleven hours, which should also be divided into three stages at different temperature ranges. However, the transformation is not complete in this case and a mixture of β and γ forms of C.I. Disperse Blue 148 is yielded. Dissimilar to the UK patent approach where the heating of an aqueous suspension of C.I. Disperse Blue 148 is carried out, our method is based upon the homogeneous recrystallization, which can overcome the shortcoming of uncompleted heterogeneous solid-to-solid crystal transformation process, and we have obtained the pure crystalline form of C.I. Disperse Blue 148.

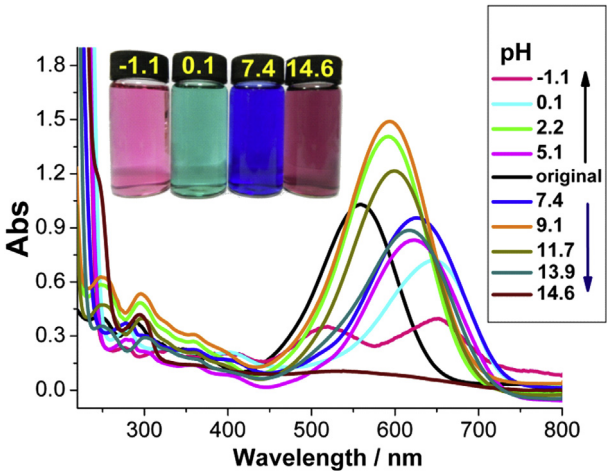

Fig. 3. UV–vis spectra of C.I. Disperse Blue 148 at different pH values starting from a concentration of 3.0×10^{-5} mol/L in methanol (the black line).

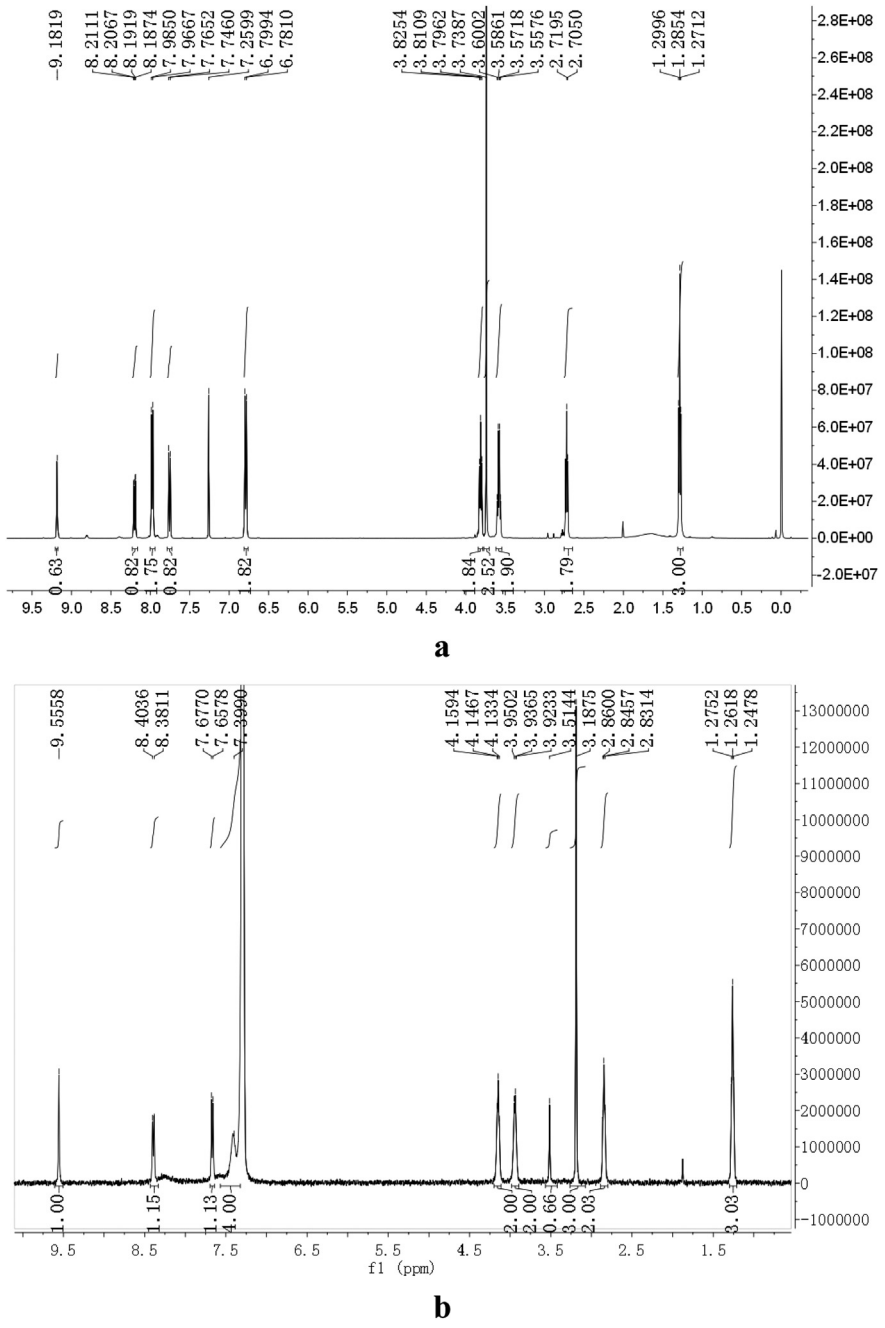

Fig. 4. Comparison on the ^{1}H NMR spectra of C.I. Disperse Blue 148 in $CDCl_3$ (a) and deuterium chloride 20% solution in D_2O (b).

It is well known that the stability, the particle size, the form of crystal and the phase purity of azo dyes are very important in the process of dyeing as well as in the "ink" used in discharge printing, especially for the high-temperature type of dyes. For example, the α form of C.I. Disperse Blue 148 (m.p. = 83–87 °C) has the worst stability and it is difficult to be grinded and kept longer, while the β form (m.p. = 88–90 °C) and the γ form (m.p. = 90–92 °C) exhibit better stability and dyeing behavior. In contrast, our reported new crystalline form of C.I. Disperse Blue 148 has the highest melting point (117–119 °C) and the best phase purity, so it would be easier for the new crystalline form of C.I. Disperse Blue 148 to be dispersed in the solid state in hot water and the best dyeing properties could be expected although many other dyeing process parameters (temperature, press, speed, time of dyeing, saturation absorption, aggregation etc) would also influence the final results. Moreover, we hope the current study of the new crystalline form of C.I. Disperse Blue 148 can provide some useful strategies for improving the dyeing properties without changing their molecular structures.

The maximum absorption wavelength of C.I. Disperse Blue 148 is centered at 588 nm in methanol (ξ = 31,690 L cm^{-1}mol^{-1}), which can be assigned as typical π–π^* transitions between the aromatic rings and the azo unit of the whole dye molecule. We have divided this solution into two parts and added concentrated hydrochloric acid and sodium hydroxide aqueous solutions, respectively, in order to adjust the pH values of mixture to study the alterations of UV–vis spectra of C.I. Disperse Blue 148.

On the one hand, as can be seen in Fig. 3, a series of variations appear when sodium hydroxide is added into the original methanol

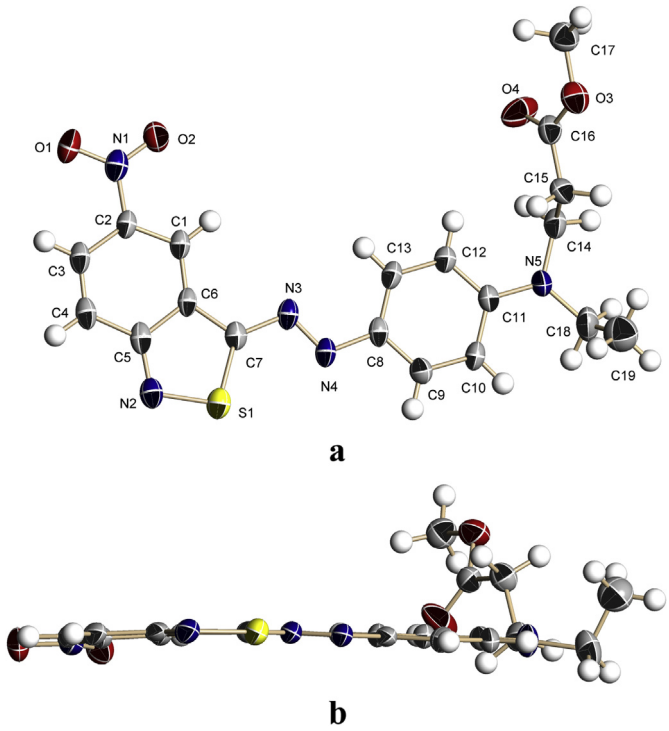

Fig. 5. ORTEP drawing of C.I. Disperse Blue 148 with the atom–numbering scheme (top view for (a) and side view for (b)). Displacement ellipsoids are drawn at the 30% probability level and the hydrogen atoms are shown as small spheres of arbitrary radii.

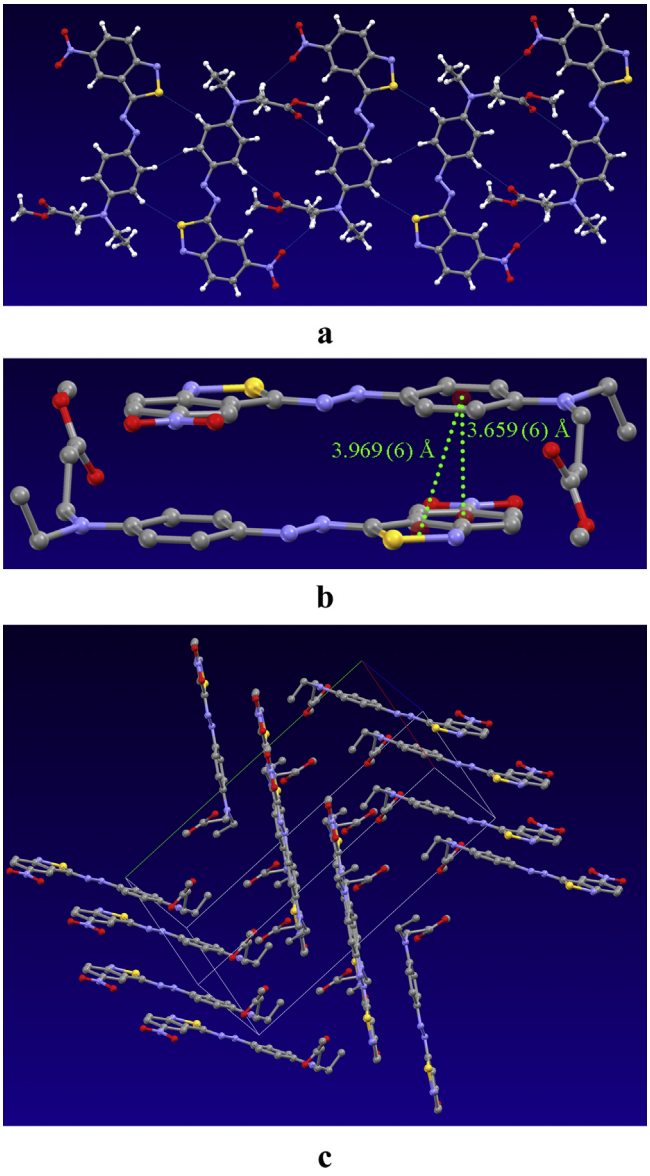

Fig. 6. Perspective view of the two-dimensional network (a), the dimeric packing mode (b), and ABAB packing fashion (c) in C.I. Disperse Blue 148.

solution of C.I. Disperse Blue 148. The maximum absorption wavelength is red-shifted to 626 nm exhibiting a bathochromic shift of 38 nm when the pH value of solution equals to 7.4. With the alkaline enhanced, the maximum absorption wavelengths of corresponding solutions are slightly blue-shifted to 593 nm (pH = 9.1), 599 nm (pH = 11.7) and 618 nm (pH = 13.9) but the molar extinction coefficients are increased in this pH value range compared with that of the original C.I. Disperse Blue 148 solution. The color of solutions does not turn from blue to dark red until the pH value of solution reaches to 14.6, and the dark red color can keep unchangeable with the addition of more sodium hydroxide. On the other hand, the color of solutions alters from blue to green (pH = 0.1) and pink (pH = −1.1) when excess hydrochloric acid is added into the original methanol solution of C.I. Disperse Blue 148. It is suggested that the changes in the absorption spectra at different pH values arise from the alterations of the conjugated system of the whole D-π-A system of dye molecule, because the protonation or deprotonation process of C.I. Disperse Blue 148 will deter or promote the electron transition between the aromatic rings and the central azo unit.

On considering that there are several possible protonation positions for C.I. Disperse Blue 148 in strong acidic condition, the ^{1}H NMR spectral comparisons on the chemical-shift variations of protons for C.I. Disperse Blue 148 are made in neutral $CDCl_3$ (Fig. 4(a)) and DCl 20% solution in D_2O (Fig. 4(b)). After the protonation of C.I. Disperse Blue 148, the chemical shifts of protons from the phenyl ring and the *N*-substituted tails are found to be significantly shifted, but the benzisothiazole protons are slightly shifted by contrast. For example, the four phenyl protons are incorporated into one broad peak, where the corresponding chemical shifts are moved from 7.97 and 6.79 ppm to 7.40 ppm, while the three benzisothiazole protons are slightly shifted from 9.18, 8.20 and 7.75 ppm to 9.56, 8.38 and 7.66 ppm. So it is concluded that the proton is added onto the nitrogen atom of *N*-substituted tails in the acidic condition instead of the benzisothiazole ring, and this protonation process will influence the conjugated system of the whole D-π-A system of dye molecule, which is suggested to be the main reason for the color change of C.I. Disperse Blue 148 at different pH values.

Further experiments reveal that the pH titration results are reversible, which means that C.I. Disperse Blue 148 is stable in strong acidic and basic conditions. Namely, the strong acidic or basic solutions of C.I. Disperse Blue 148 in green or red can return to blue by adding proper amounts of acid or base to neutralize the solutions. In addition, a single peak at 3.19 ppm in DCl 20% solution in D_2O indicates the presence of these three protons of methyl ester ($COOCH_3$), indicative of the stability of C.I. Disperse Blue 148 in strong acidic condition. Actually, fibers can keep unchangeable for a long time in the conventional acidic and basic conditions (pH = 4–9), since it is difficult for an acid or a base to touch the disperse dye molecules once they have entered the fibers. In this work, we aim to examine the color shift of C.I. Disperse Blue 148 under the extremely strong acidic and basic conditions just for the need of

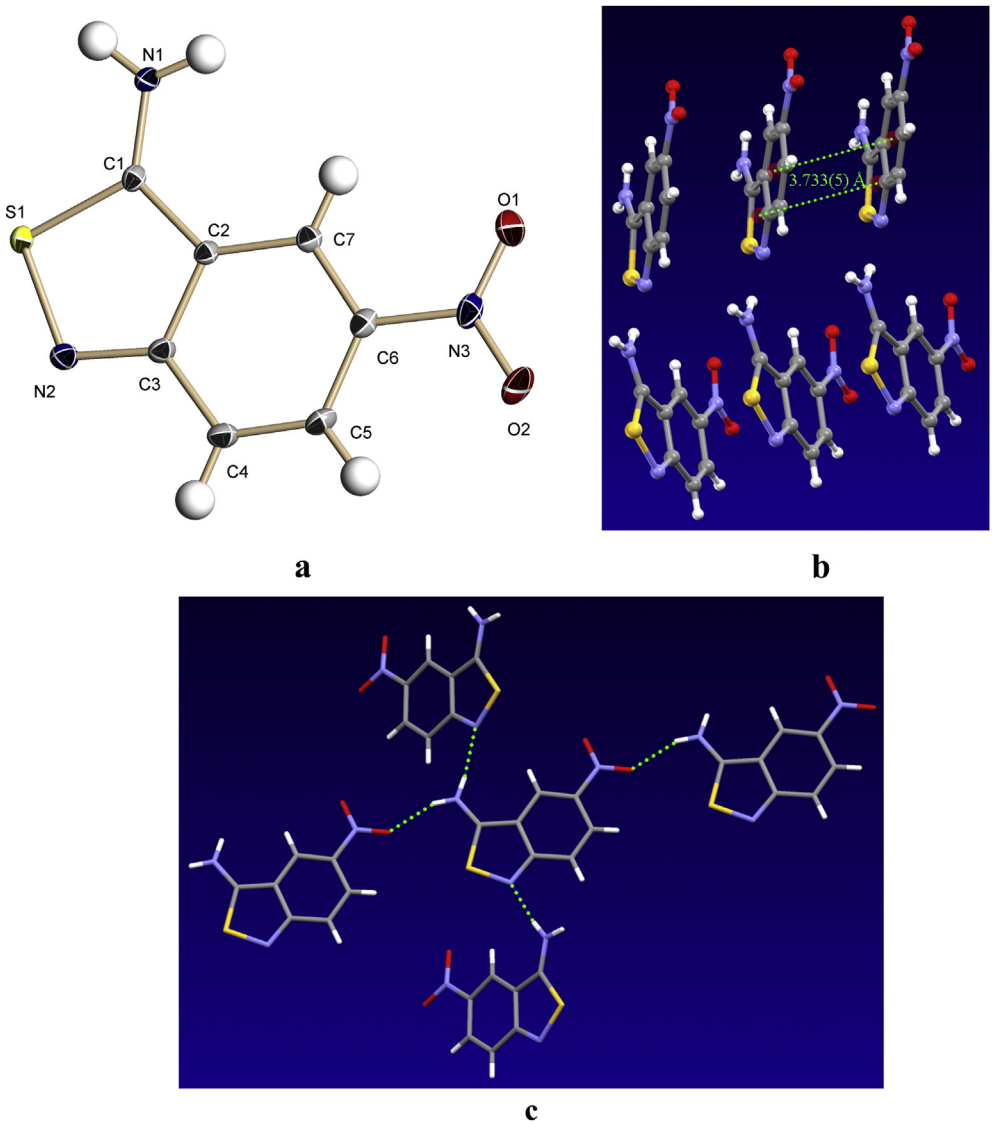

Fig. 7. (a) ORTEP drawing of **1** with the displacement ellipsoids at the 30% probability level and the hydrogen atoms shown as small spheres of arbitrary radii. (b) and (c) Perspective view of the offset π–π stacking and hydrogen bonding interactions between adjacent molecules in **1**.

theoretical research, which is indeed hard to reach in the real dyeing and washing processes.

3.2. Structural description of C.I. Disperse Blue 148 and 3-amino-5-nitro-[2,1]-benzisothiazole (*1*)

The molecular structure of C.I. Disperse Blue 148 with atom-numbering scheme is shown in Fig. 5(a). It crystallizes in the monoclinic $P2_1/c$ space group without the presence of any solvent molecule. The sulfur atom of benzisothiazole ring is found to be the same side of azo unit. As a common feature of azo dyes, the dihedral angle between the phenyl and the isothiazole ring is 2.7(5)°, exhibiting good planarity of the whole molecule. As shown in Fig. 5(b), all the non-hydrogen atoms except the *N*-substituted tails in C.I. Disperse Blue 148 are essentially coplanar with the mean deviation from least-squares plane of 0.065(6) Å. Both of the *N*-substituted groups lie on the same side of molecular plane.

In the crystal packing of C.I. Disperse Blue 148, weak intermolecular C–H···O hydrogen bonding interactions can be observed between neighboring molecules constituting a two-dimensional laminar network (Fig. 6(a)). It is noted that a dimeric packing structure with weak offset π–π stacking interactions is found between adjacent phenyl and benzisothiazole rings of different molecules. The centroid-to-centroid separations between them are 3.659(6) and 3.969(6) Å, respectively, as shown in Fig. 6(b). The two molecules adopt a head-to-tail arrangement where the *N*-substituted groups are positioned at the same side of each molecule in the dimeric unit pointing to their counterparts. In addition, there are two sets of molecules in the packing structure of C.I. Disperse Blue 148 (the ABAB packing fashion) with the dihedral angle of 63.3(5)o between them, as shown in Fig. 6(c).

By checking the latest version of CCDC database (updated to August 2012), it is found that there are only three structural reports [27–29] on five triazene compounds having the common [2,1]-benzisothiazole unit. However, no structural examples can be found on neither [2,1]-benzisothiazole nor [1,2]-benzisothiazole based azo dyes. So it is suggested that C.I. Disperse Blue 148 is the first structural instance on this family of compounds.

The molecular structure of **1** with atom-numbering scheme is shown in Fig. 7(a). The X-ray single-crystal diffraction analysis for **1**

reveals that all the atoms are essentially coplanar with the mean deviation from least-squares plane of 0.043(4) Å. A reasonable Flack parameter of −0.05(13) indicates the correct assignment of the monoclinic non-centrosymmetric *Pn* space group. As can be seen in Fig. 7(b), weak offset π−π stacking interactions are found between adjoining benzisothiazole rings with the centroid-to-centroid contacts of 3.733(5) Å. There are also two sets of molecules in the crystal packing with the dihedral angle of 42.0(3)o between them. Furthermore, every 3-amino-5-nitro-[2,1]-benzisothiazole molecule is linked by four adjacent ones via the intermolecular N–H···N and N–H···O hydrogen bonding interactions (Table 3) between the two hydrogen atoms of amino group and the nitrogen atom of imidazole ring and one oxygen atom of nitro group, respectively (Fig. 7(c)). As a result, a three-dimensional supramolecular framework is constructed in **1** with the help of afore-mentioned π−π stacking and hydrogen bonding interactions.

4. Conclusion

In summary, we have described herein the structural and spectral characterizations of C.I. Disperse Blue 148, which is a famous high-temperature trichromatic blue azo dye widely used in cellulose acetate. An essentially planar molecular structure is observed where a novel complementary dimeric head-to-tail packing structure is formed. It is noted that a new crystalline form of C.I. Disperse Blue 148 is obtained, which is consistent with the simulative curve calculated from the single-crystal diffraction data. This new crystalline form is obtained by a homogeneous recrystallization method in the replacement of an uncompleted heterogeneous solid-to-solid crystal transformation process by heating an aqueous suspension of α form of C.I. Disperse Blue 148 mentioned in a UK patent. Compared with the known α, β, and γ forms of C.I. Disperse Blue 148, this new crystalline form obtained by a complete solvent-assisted transformation method shows the highest melting point at 117–119 °C and the best thermal stability. Furthermore, the pH titration experiments have been carried out to reveal the pH stability of this heterocyclic monoazo dye, where the ^{1}H NMR spectral comparisons of C.I. Disperse Blue 148 in neutral $CDCl_3$ (Fig. 4(a)) and DCl 20% solution in D_2O (Fig. 4(b)) are performed to show the chemical-shift variations of protons and reveal the influence of protonation process on the color change of C.I. Disperse Blue 148 at different pH values.

As far as we are aware, C.I. Disperse Blue 148 is the first structural example on benzisothiazole based azo dyes. On considering the tremendous gap that still exists between the structures and the properties for dye molecules, we hope the structural spectral and crystal transformation studies for this high-performance blue dye can throw some new light on the design, effective molecular screening and possible application of new aromatic heterocyclic azo dyes.

Acknowledgments

This work was supported by the Major State Basic Research Development Programs (Nos. 2013CB922101, 2011CB933300 and 2011CB808704), the National Natural Science Foundation of China (Nos. 21171088 and 21021062) and Qing Lan Project.

Appendix A. Supplementary data

Supplementary data related to this article can be found at http://dx.doi.org/10.1016/j.dyepig.2013.06.002.

References

[1] Neamtu M, Yediler A, Siminiceanu I, Macoveanu M, Kettrup A. Decolorization of disperse red 354 azo dye in water by several oxidation processes-acomparative study. Dyes Pigm 2004;60:61–8.
[2] Towns AD. Developments in azo disperse dyes derived from heterocyclic diazo components. Dyes Pigm 1999;42:3–28.
[3] Freeman HS, Posey JC. An approach to the design of lightfast disperse dyes-analogs of Disperse Yellow 42. Dyes Pigm 1992;20:171–95.
[4] Shi QQ, Sun R, Ge JF, Xu QF, Li NJ, Lu JM. A comparative study of symmetrical and unsymmetrical trimethine cyanine dyes bearing benzoxazolyl and benzothiazolyl groups. Dyes Pigm 2012;93:1506–11.
[5] Maradiya HR, Patel VS. Monomeric and polymeric disperse dyes based on heterocyclic compound for hydrophobic fabric. Polym-Past Technol Eng 2002;41:735–49.
[6] Maradiya HR, Patel VS. Dyeing performance of disperse dyes based on 2-aminothiazole for cellulose triacetate and nylon fibers. Fiber Polym 2002;3:43–8.
[7] You W, Zhu HY, Huang W, Hu B, Fan Y, You XZ. The first observation of azohydrazone and *cis-trans* tautomerisms for Disperse Yellow dyes and their nickel(II) and copper(II) complexes. Dalton Trans 2010;39:7876–80.
[8] Hu B, Wang G, You W, Huang W, You XZ. Azo-hydrazone tautomerism by *in situ* Cu(II) ion catalysis and complexation with the H_2O_2 oxidant of C.I. Disperse Yellow 79. Dyes Pigm 2011;91:105–11.
[9] Huang W. Structural and computational studies of azo dyes in the hydrazone form having the same pyridine-2,6-dione component (II): C.I. Disperse Yellow 119 and C.I. Disperse Yellow 211. Dyes Pigm 2008;79:69–75.
[10] Qian HF, Huang W. An azo dye molecule having a pyridine-2,6-dione backbone. Acta Crystallogr C-Cryst Str 2006;62:o62–4.
[11] Huang W, Qian HF. Structural characterization of C.I. Disperse Yellow 114. Dyes Pigm 2008;77:446–50.
[12] Chen XC, Tao T, Wang YG, Peng YX, Huang W, Qian HF. Azo-hydrazone tautomerism observed from UV-vis spectra by pH control and metal-ion complexation for two heterocyclic Disperse Yellow dyes. Dalton Trans 2012;41:11107–15.
[13] Tao T, Xu F, Chen XC, Liu QQ, Huang W, You XZ. Comparisons between azo dyes and schiff bases having the same benzothiazole/phenol skeleton: syntheses crystal structures and spectroscopic properties. Dyes Pigm 2012;92:916–22.
[14] Chen XC, Wang YG, Tao T, Huang W, Qian HF. Two pairs of 1:2 nickel(II) and copper(II) metal-complex dyes showing the same *trans* configuration and azo-hydrazone transformation but different thermal properties. Dalton Trans 2013;42:7679–92.
[15] Geng J, Tao T, You W, Huang W. Structural investigations on four heterocyclic Disperse Red azo dyes having the same benzothiazole/azo/benzene skeleton. Dyes Pigm 2011;90:65–70.
[16] BASF. DE Patent 1,544,375, 1965.
[17] Whitham C, Buckley AJ, Crowson RJ. Dye composition. US Patent 6,365,718 B1, 2002.
[18] BASF. Novel modifications of a disperse monoazo dye which are stable under dyeing conditions. UK Patent 1,438,586, 1976.
[19] Qiu FX, Zhou YM, Liu JZ, Zhang XP. Preparation, morphological and thermal stability of polyimide/silica hybrid material containing dye NBDPA. Dyes Pigm 2005;71:37–42.
[20] Tauber MM, Cavaco-Paulo A, Robra KH, Gubitz GM. Nitrile hydratase and amidase from *Rhodococcus rhodochrous* hydrolyze acrylic fibers and granular polyacrylonitriles. Appl Environ Microbiol 2000;66:1634–8.
[21] Phillips D, Suesat J, Taylor JA, Wilding M, Farrington D, Bone J, et al. Thermal migration of selected disperse dyes on poly(ethylene terephthalate) and poly(lactic acid). Color Technol 2004;120:260–4.
[22] Kraska J, Sokolowska-Gajda J. Properties of monoazo disperse dyes derived from 3-amino-5-nitro(2,1)benzisothiazole. J Soc Dyers Colour 1984;100:316–9.
[23] Siemens. SAINT v4 software reference manual. Madison, Wisconsin, USA: Siemens Analytical X-Ray Systems, Inc.; 2000.
[24] Sheldrick GM. SADABS, program for empirical absorption correction of area dectector data. Germany: Univ. of Gottingen; 2000.
[25] Siemens. SHELXTL, version 6.10 reference manual. Madison, Wisconsin, USA: Siemens Analytical X-Ray Systems, Inc.; 2000.
[26] Georgiadou KL, Tsatsaroni EG, Kehayoglou AH. Synthesis and characterization of hetarylazo disperse dyes derived from substituted N-β-acetoxyethylanilines—application on cellulose acetate. J Appl Polym Sci 2004;92:3479–83.
[27] Prikryl J, Lycka A, Bertolasi V, Holcapek M, Machacek V. Structure and reactivity of 3,3-disubstituted 1-(5-nitro-2,1-benzisothiazol-3-yl)triazenes. Eur J Org Chem 2003:4413–21.
[28] Prikryl J, Machacek V, Jansa P, Svobodova M, Ruzicka A, Nachtigall P, et al. Stable triazenes derived from 2-alkylaminonaphthalenes and 5-nitrobenzo[c]-1,2-thiazole-3-diazonium hydrogensulfate. Eur J Org Chem 2008:3272–8.
[29] Kettmann V, Lokaj J, Kozisek J, Prikryl J, Machacek V. 3-Butyl-1-(5-nitrobenzo[c][1,2]-thiazol-3-yl)-3-phenyltriazene. Acta Crystallogr C-Cryst Str 2004;60:o143–5.